



September 14, 1990

Warsaw University Preprint *IFD/7/1990*

SCALING OF MULTIPLICITY DISTRIBUTIONS AND COLLISION DYNAMICS IN e^+e^- AND pp INTERACTIONS

M. Gaździcki, R. Szwed, G. Wrochna and A.K. Wróblewski

Institute of Experimental Physics

Warsaw University

PL-00-681 Warsaw, ul. Hoża 69

Abstract

The scaling properties of multiplicity distributions for e^+e^- and pp collisions are summarized. It is shown that in both cases the distributions have a lognormal shape.

Possible relations between e^+e^- and pp collision dynamics are discussed in a framework of scaling properties of multiplicity distributions. The form of the energy dependence of mean multiplicity is obtained as a consequence of the multiplicity scaling.

1 Introduction

Scaling properties of multiplicity distributions in pp inelastic collisions were established many years ago [1,2,3]. However only recently the new experimental data [4,5] allowed to study the properties of multiplicity distributions in e^+e^- interactions in the energy range and with the precision comparable with those for the pp case. It was shown [6] that the KNO-G scaling [2,3], established for pp collisions, holds also for e^+e^- interactions. The KNO-G scaling properties, the lognormal form of the scaling function, and the energy dependence of the mean multiplicity observed in e^+e^- interactions can be explained assuming a simple scale invariant branching process [7] as the mechanism of multiparticle production.

The proton in contrary to the electron is not a point-like object. It consist of quarks, antiquarks and gluons. It is therefore natural to treat e^+e^- interaction as a basic elementary process and try to understand more complex process, such as pp collision, as a combination of e^+e^- -like elementary processes.

In this paper we show that also in the case of pp collisions the multiplicity distribution has the lognormal shape. Further we discuss possible constructions of pp collisions from e^+e^- interactions which provide the KNO-G scaling as required by the experimental data. Those constructions are possible provided that the mean multiplicity has a power dependence on the available energy for both e^+e^- and pp interactions which is consistent with the experimental data.

The paper is organized as follows. Basic properties of multiplicity distributions in e^+e^- and pp collisions are summarized in Section 2. The possible constructions of pp collisions from e^+e^- -like processes are presented in Section 3. Summary and discussion are given in Section 4.

2 Comparison of multiplicity distributions in pp and e^+e^- collisions

The multiplicity distributions for e^+e^- and pp collisions (except¹ the UA5 $p\bar{p}$ data at 540 GeV) obey the KNO-G scaling [2,3,6]:

$$P_n = \int_0^{n+1} P(\bar{n}) d\bar{n}, \quad (2.1)$$

$$P(\bar{n}) = \frac{1}{\langle \bar{n} \rangle} \psi \left(\frac{\bar{n}}{\langle \bar{n} \rangle} \right). \quad (2.2)$$

Here P_n denotes the probability to have an inelastic collision² with n produced pairs of charged particles, $\psi(z)$ is called a scaling function, and $\langle \bar{n} \rangle$ is a continuous average multiplicity:

$$\langle \bar{n} \rangle = \int_0^\infty \bar{n} P(\bar{n}) d\bar{n}. \quad (2.3)$$

¹The $p\bar{p}$ data at 540 GeV are used in this paper as pp data at this energy.

²The nondiffractive pp collisions were independently studied in Ref. [8].

The standard test of the scaling [2,3] is presented in Fig. 1 for pp and e^+e^- interactions. The sum $S_n = \sum_{i=1}^n P_i$ is plotted as a function of $z = n/\langle \bar{n} \rangle$. The data points from different energies lie on the same curve which shows validity of the scaling for both data sets, e^+e^- and pp . The c.m. energy range covered by the presented data is from 3 to 91 GeV for e^+e^- and from 3 to 62 GeV for pp collisions.

The scaling function $\psi(z)$ for e^+e^- interactions was found to have a lognormal form [6,13] as suggested by the multiplicative nature of the process [7]. It is interesting that also the pp data can be described by lognormal probability density, but with the parameters different from those in the e^+e^- case. For the lognormal distribution the scaling function takes the form

$$\psi(z) = \frac{N}{\sqrt{2\pi}\sigma} \cdot \frac{1}{z+c} \exp \left(-\frac{[\ln(z+c) - \mu]^2}{2\sigma^2} \right). \quad (2.4)$$

The parameters N, μ, c and σ are constrained by the two normalization conditions³

$$\sum_0^\infty P_n = \int_0^\infty P(\bar{n}) d\bar{n} = \int_0^\infty \psi(z) dz = \frac{N}{2} \operatorname{erfc} \left(\frac{\ln c - \mu}{\sqrt{2}\sigma} \right) = 1, \quad (2.5)$$

$$\langle z \rangle = \int_0^\infty z \psi(z) dz = R \cdot \exp \left(\mu + \frac{\sigma^2}{2} \right) - c = 1 \quad (2.6)$$

where

$$R = \frac{\operatorname{erfc}(\nu - \sigma/\sqrt{2})}{\operatorname{erfc}(\nu)} \quad \text{and} \quad \nu = \frac{\ln c - \mu}{\sqrt{2}\sigma}. \quad (2.7)$$

In practice it is best to choose as fit parameters the shift c and the dispersion of the scaling function D

$$D = \left(\int_0^\infty (z - \langle z \rangle)^2 \psi(z) dz \right)^{1/2} \quad (2.8)$$

and then calculate N, μ and σ from the above normalization conditions and the definition of D . Other choice may produce strong correlation between parameters. The details can be found in Ref. [9].

We have fitted in this way the lognormal distribution separately to each pp data set between $\sqrt{s} = 3$ and 540 GeV [10]. The results are given in Table 1. The value of the χ^2/NDF is of the order of 1 for all data sets except the two sets published by V. Blobel et al. [10]. The reason is that those data are based on very large statistics and the statistical errors are probably smaller than the systematic ones. Thus the χ^2 value calculated from the statistical errors is relatively large but the experimental distributions can agree with the lognormal one within the range of systematic errors. The resulting values of parameters c and D are also plotted in Fig. 1. Some statistical fluctuations are seen but there is no systematic dependence of the parameters on the energy. Only the value of c for the UA5 data is significantly lower than the others. The results suggest that all data in the range from $\sqrt{s} = 3$ to 62 GeV can be described by a single lognormal distribution with two fixed parameters.

We have found these parameters by fitting a lognormal distribution to all data from this range simultaneously. The fit gave

³We assume that $c > 0$. If $c \leq 0$ then $N = 1$ and in the next formula $R = 1$.

$$\alpha = 0.459 \pm 0.002, \quad \beta_{ee} = 1.390 \pm 0.009 \quad \beta_{pp} = 0.888 \pm 0.007, \quad (2.14)$$

$$(\chi^2/NDF = 211/148 = 1.43)$$

fitted simultaneously to all the e^+e^- and pp data points. The UA5 pp data was not included to the fit. The function reproduces the data satisfactorily.⁴ This means that the dependence of the average multiplicity on the energy in pp interactions is the same as in e^+e^- collisions if the available energy is divided by a factor $\gamma = (\beta_{ee}/\beta_{pp})^{1/\alpha} = 2.65$.

Let us summarize the properties of the data.

- (i) The multiplicity distributions for the e^+e^- and pp interactions obey the KNO-G scaling.
- (ii) The scaling function has a lognormal form, however the values of the parameters are different for the e^+e^- and pp data.
- (iii) The continuous mean multiplicity depends on the available energy W as W^α where the exponent α is identical for the e^+e^- and pp data.

3 Proton-proton collisions as a combination of elementary processes

The structure of the proton makes multiparticle production in pp collisions more complicated than in e^+e^- interactions. Various models take this fact into account in a different way. We do not intend to propose here another model, competitive to the existing ones. Instead we would like to extract basic assumptions, common for various models, which correctly describe discussed phenomena. Most models consider one of the two scenarios presented below or a certain combination of both.

Scenario 1. Only one parton from each proton is engaged in the reaction, whereas the remaining partons are only "spectators". Thus, the colliding partons initiate a process similar to that in the e^+e^- collisions. However, the spectators remove a part of the energy so that the initial energy of the cascade varies from event to event. Thus, the final distribution is a mixture of the elementary distributions with various initial energies.

Scenario 2. The initial energy is divided among a number of colliding parton pairs. Each pair develops an elementary process. Thus, the final distribution is a convolution of several elementary distributions. Let us discuss in detail these two scenarios.

Ad scenario 1

Let us denote the CMS energy of the colliding partons, i.e. the energy available for multiparticle production, by κW . (κ is sometimes called an inelasticity.) If we denote the distribution of κ by $f(\kappa, W)$ the multiplicity distribution for pp collisions is given by the formula

$$P_n^{pp}(W) = \int_0^1 f(\kappa, W) P_n^{ee}(\kappa W) d\kappa. \quad (3.1)$$

The above formula can be rewritten using scaling functions ψ for e^+e^- and pp collisions

⁴It is to be remembered that published data on hadrons multiplicities in e^+e^- interactions usually include also products of weak decays of K^0, Λ and other particles with lifetime $\sim 10^{-10}$ s.

$$c = 4.25 \pm 0.20, \quad D = 0.629 \pm 0.003 \quad \chi^2/NDF = 458/316 = 1.45. \quad (2.9)$$

$$(N = 1.061 \quad \mu = 1.638 \quad \sigma = 0.1210)$$

Partial values of χ^2 are also given in Tab. 1. The resulting lognormal distribution together with the experimental data is presented in Fig. 2 which is the so called probit diagram [7, 11, 12]. The agreement of the data with the straight line representing the fitted distribution proves the scaling and the lognormal shape of measured distributions. The shapes of the scaling function for pp and e^+e^- collisions are compared in Fig. 3. We recall here the values of the parameters of lognormal distribution fitted to e^+e^- data [4]

$$e^+e^-: \quad c = 0.56 \pm 0.03, \quad D = 0.277 \pm 0.001 \quad \chi^2/NDF = 208/285 = 0.74, \quad (2.10)$$

$$(N = 1.000 \quad \mu = 0.429 \quad \sigma = 0.1762) \quad [13]$$

As it was mentioned earlier, the fit to the UA5 data at 540 GeV yielded parameters slightly different from the result obtained for the lower energy data

$$c = 1.12 \pm 0.22, \quad D = 0.642 \pm 0.011 \quad \chi^2/NDF = 29/38 = 0.77 \quad (2.11)$$

$$(N = 1.028 \quad \mu = 0.692 \quad \sigma = 0.3003).$$

To make direct comparison we have plotted the UA5 multiplicity distribution together with both curves in Fig. 4. The continuous line represents the fit to the UA5 data and the dotted one — to the lower energy data. It is seen that the scaling violation is significant, but less than in nondiffractive collisions which is often quoted. Unfortunately multiplicity distributions in inelastic pp collisions at 200 and 900 GeV were not published until now.

An alternative test of the scaling is presented in Fig. 5 where the dispersions of various orders

$$D_k = \left(\langle n^k \rangle - \langle n \rangle^k \right)^{1/k} \quad (2.12)$$

are plotted as a function of the average charge multiplicity $\langle n_{ch} \rangle$ for pp and e^+e^- interactions. The continuous lines are calculated from the lognormal distribution (2.9).

Thus, all multiplicity distributions in pp inelastic collisions can be described by a single lognormal distribution with two parameter fixed for all energies except for the UA5 data which can be described also by a lognormal distribution but with slightly different parameters.

To compare the dependence of the average multiplicity on the energy in the pp and e^+e^- interactions we should note that for pp collisions only the available energy $W = \sqrt{s} - 2m_p$ (m_p is a proton mass), rather than \sqrt{s} can be spent for particle production. This correction is not important at high energies, but could not be neglected in the region of $\sqrt{s} \leq 20$ GeV. It is also recommended [3] to use the continuous average multiplicity $\langle \bar{n} \rangle$ (for $\langle n_- \rangle \gtrsim 1$ one can use the approximation: $\langle \bar{n} \rangle = \langle n_- \rangle + 0.5$).

The dependence of $\langle \bar{n} \rangle$ on W for the e^+e^- and pp collisions is shown in Fig. 6. We start from $\langle \bar{n} \rangle \gtrsim 2$ to avoid problems coming from trigger definition. The straight lines represent the function

$$\langle \bar{n} \rangle = \begin{cases} \beta_{ee} W^\alpha & \text{for } e^+e^- \\ \beta_{pp} W^\alpha & \text{for } pp \end{cases} \quad (2.13)$$

with parameters

$$\frac{1}{\langle \bar{n}^{pp} \rangle(W)} \psi^{pp} \left(\frac{n}{\langle \bar{n}^{pp} \rangle(W)} \right) = \int_0^1 f(\kappa, W) \frac{1}{\langle \bar{n}^{ee} \rangle(\kappa W)} \psi^{ee} \left(\frac{n}{\langle \bar{n}^{ee} \rangle(\kappa W)} \right) d\kappa. \quad (3.2)$$

Denoting

$$z = \frac{n}{\langle \bar{n}^{pp} \rangle(W)}, \quad R(\kappa, W) = \frac{\langle \bar{n}^{pp} \rangle(W)}{\langle \bar{n}^{ee} \rangle(\kappa W)} \quad (3.3)$$

we can rewrite formula (3.2) in a simplified form

$$\psi^{pp}(z) = \int_0^1 f(\kappa, W) R(\kappa, W) \psi^{ee}(z \cdot R(\kappa, W)) d\kappa. \quad (3.4)$$

The scaling function $\psi^{pp}(z)$ will be independent of the energy W for any non-negative functions f , R , and ψ^{ee} provided that $f(\kappa, W)$ and $R(\kappa, W)$ are independent of W . This means that $f(\kappa, W) \equiv f(\kappa)$ and the energy dependence of the numerator and the denominator of R should cancel. In general it is possible only if the continuous average multiplicity depends on the energy W according to a power law:

$$\langle \bar{n} \rangle(W) = \beta W^\alpha \quad (3.5)$$

where the power α is identical for e^+e^- and pp collisions.

Ad scenario 2

Let us assume that the CMS energy of colliding protons, W , is distributed uniformly among k colliding parton pairs. Thus each pair develops an elementary process with the initial energy W/k . We denote by $g(k, W)$ the probability that k parton-parton collisions take place in a given event. Then the multiplicity distribution for pp collisions is given by

$$F_n^{pp}(W) = \sum_{k=1}^{\infty} g(k, W) F_n^{ee}(W/k)^{*k} \quad (3.6)$$

where the superscript $*k$ denotes a k -fold convolution.

Let us first discuss the multiplicity distribution for a fixed number of elementary processes

$$F_{n|k}^{pp}(W) = F_n^{ee}(W/k)^{*k}. \quad (3.7)$$

The average of the k -fold convolution is k times greater than the average of the elementary process, therefore

$$\langle \bar{n}^{pp} \rangle_k(W) = k \langle \bar{n}^{ee} \rangle(W/k). \quad (3.8)$$

To check the scaling properties we use the characteristic function defined as

$$\varphi_x(t) = \langle e^{itx} \rangle \quad (3.9)$$

where x is a random variable. We take advantage of the fact that

$$\varphi_{ax}(t) = \langle e^{itax} \rangle = \varphi_x(at). \quad (3.10)$$

For the scaling function we have

$$\psi \left(\frac{n}{\langle \bar{n} \rangle} \right) \rightarrow \varphi_{n/\langle \bar{n} \rangle}(t) = \varphi_n \left(\frac{t}{\langle \bar{n} \rangle} \right) \quad (3.11)$$

This means that in terms of the characteristic function the scaling consists in dividing the variable t by the factor $\langle \bar{n} \rangle$. The characteristic function of the convolution is given by the product of elementary characteristic functions

$$\varphi_n^{*k} \left(\frac{t}{\langle \bar{n} \rangle} \right) = \varphi_n^k \left(\frac{t}{\langle \bar{n} \rangle} \right) \quad (3.12)$$

Using Eq. (3.8) we can write

$$\varphi_n^{*k} \left(\frac{t}{\langle \bar{n} \rangle} \right) = \varphi_n^k \left(\frac{kt}{\langle \bar{n} \rangle^{*k}} \right) \quad (3.13)$$

We see that the argument of the characteristic function of the convolution has again the form $t/\langle \bar{n} \rangle^{*k}$, i.e. the convolution operation preserves the scaling.

Let us denote the scaling function of the distribution $F_{n|k}^{ee}(W)$ by $\psi_k^{pp}(n/\langle \bar{n}^{pp} \rangle_k)$. Similarly to the Scenario 1 one can rewrite the formula (3.6) in terms of scaling functions

$$\psi^{pp}(z) = \sum_{k=1}^{\infty} g(k, W) Q(k, W) \psi_k^{pp}(z \cdot Q(k, W)) \quad (3.14)$$

where

$$Q(k, W) = \frac{\langle \bar{n}^{pp} \rangle(W)}{k \langle \bar{n}^{ee} \rangle(W/k)} \quad (3.15)$$

Just as in Scenario 1 the function $\psi^{pp}(z)$ is energy independent provided that $g(k, W) \equiv g(k)$ and $\langle \bar{n} \rangle = \beta W^\alpha$ where the power α is identical for e^+e^- and pp collisions.

Let us now discuss a process which is a combination of Scenarios 1 and 2. In this case a part of the available energy is randomly divided among a random number of elementary processes. Denoting by $f(\kappa, k, W)$ an inelasticity distribution of the elementary process for an event with k processes we get

$$F_n^{pp}(W) = \sum_{k=1}^{\infty} g(k, W) \left[\int_0^1 f(\kappa, k, W) F_n^{ee}(\kappa W) \right]^{*k} \quad (3.16)$$

provided that the correlation between elementary processes due to the energy conservation can be neglected. Repeating the considerations presented in Scenarios 1 and 2 we obtain the same conclusions.

Let us now summarize the results obtained in both scenarios under the requirement imposed by the experimental data that in e^+e^- and pp collisions the KNO-G scaling holds.

A. The continuous mean multiplicity is proportional to W^α , where the exponent α is the same for e^+e^- and pp collisions. This result is common for both scenarios.

B. The inelasticity distribution (Scenario 1) or the distribution of the number of elementary sources (Scenario 2) are energy independent. In the case of the combination of the two scenarios both distributions have to be energy independent.

4 Summary and discussion

It has been shown that multiplicity distributions in pp collisions have properties similar to those observed in e^+e^- interactions. The distributions obey the scaling, the shape of the distribution is lognormal, and the average multiplicity depends on the energy according to a power law. It is natural to suppose that pp interactions are a certain combination of elementary processes similar to the e^+e^- collisions. In the recent years many explanations of pp data along this line have been proposed. However, the starting point, i.e. the multiplicity distribution in e^+e^- collisions, was not well defined, because of the poor quality of the available data. When the precision e^+e^- data [4] were published, a detailed analysis became possible.

In the present paper we have specified a class of models which give the scaling in pp collisions as a consequence of the scaling in e^+e^- interactions and of the partonic structure of the proton. The following picture was considered: A part of the energy of colliding particles may be distributed randomly among a random number of colliding parton pairs. Then, each pair independently develops an elementary process, similar to that in the e^+e^- collisions.

The requirement, given by the experimental data, that the KNO-G scaling holds for both e^+e^- and pp collisions connected by the above picture leads to the energy independence of probability distributions used in the analysis and to a power dependence of the mean multiplicity on the available energy with the same exponent for the e^+e^- and pp interactions. This dependence is confirmed by the experimental data. It is worthwhile to mention that this dependence was also obtained for the e^+e^- interactions analysed in terms of scale invariant bivariate branching [7] together with the scaling and with the lognormal form of the distribution.

It is interesting why the multiplicity distributions in pp collisions are also lognormal. It is not seen directly from the above considerations. We can give here only some qualitative arguments. The lognormal shape of the multiplicity distributions in the e^+e^- collisions was derived in Ref. [7] by applying the Central Limit Theorem to the stochastic process of particle production. It means that the final distribution depends on the general features of the process rather than on the details concerning individual vertices. In the case of pp collisions the initial interaction (Scenario 1 or 2) can be treated as a first step of the branching. Of course this step has slightly different properties than the remaining steps but (due to the Central Limit Theorem) it can only change the parameters of the final distributions.

Finally we would like to mention that the approach presented here is so general that it can be valid also in nuclear collisions.

References

- [1] Z.Koba, H.B.Nielsen and P.Olesen: Nucl. Phys. B40 (1972) 317.
- [2] A.I.Golokhvastov: Sov. J. Nucl. Phys. 27 (1978) 430; 30 (1979) 128.
- [3] R.Szwed and G.Wrochna: Z. Phys. C29 (1985) 255.
- [4] LENA (7.4, 8.9, 9.3 GeV) B.Niczyporuk et al.: Z. Phys. C9 (1981) 1;
JADE (12, 30, 35 GeV) W.Bartel et al.: Z. Phys. C20 (1983) 187;
HRS (29 GeV) M.Derrick et al.: Phys. Rev. D34 (1986) 3304;

TASSO (14.0, 22.0, 34.8, 43.6 GeV) W.Braunschweig et al.: Z. Phys. C45 (1988) 1939;
AMY (50.0, 52.0, 55.0, 56.0, 57.0, 60.0, 60.8, 61.4 GeV) H.W.Zheng et al.: Phys. Rev. D42 (1990) 737; DELPHI (91 GeV) DELPHI collaboration: CERN-PPE/90-117.

- [5] MARK I (2.6-6.3 GeV) J.L.Siegrist et al.: Phys. Rev. D26, (1982) 969;
CLEO (10.5 GeV) M.S.Alam et al.: Phys. Rev. Lett. 49 (1982) 357;
PLUTO (9.4, 12.0, 13.0, 17.0, 22.0, 27.5, 30.6 GeV) Ch.Berger et al.: Phys. Lett. 95B (1980) 313;
TOPAZ (52.5, 55.5 GeV) Proc. of the XXIV Int.Conf. on HEP (Springer-Verlag, 1988);
MARK II (91 GeV) Phys. Rev. Lett. 64 (1990) 1334;
ALEPH (91 GeV) D.Decamp et al.: Phys. Lett. 234B (1990) 209.
- [6] R.Szwed and G.Wrochna: Z. Phys. C47 (1990) 449.
- [7] R.Szwed, G.Wrochna and A.K.Wróblewski: Mod. Phys. Lett. A23 (1990) 1851.
- [8] G.Engelmann, S.Carius: "Multiplicity Distribution from Cascade Processes", Uppsala University preprint TSL-ISV:32, to be published in the Proceedings of the XXVth Rencontres de Moriond "High Energy Hadronic Interactions", Les Arcs, France, March 1990.
- [9] G.Wrochna: "How to Fit the Lognormal Distribution", Warsaw University Preprint IFD/8/1990.
- [10] 4.0 GeV/c, L.Bodini et al.: Nuovo Cim. 58A (1968) 475;
5.5 GeV/c, G.Alexander et al.: Phys. Rev. 154 (1967) 1284;
6.6 GeV/c, E.R.Gellert et al.: LBL-749 (1972);
12.0 GeV/c, V.Blobel et al.: Nucl. Phys. B69 (1974) 454;
19.0 GeV/c, H.Boggild et al.: Nucl. Phys. B41 (1972) 285;
24.0 GeV/c, V.Blobel et al.: Nucl. Phys. B52 (1975) 221;
35.7 GeV/c, I.V.Bogulavsky et al.: JINR-10134 (1976);
50.0 GeV/c, V.V.Ammosov et al.: Phys. Lett. 42B (1972) 519;
60.0 GeV/c, C.Bromberg et al.: Phys. Rev. D15 (1977) 64;
69.0 GeV/c, V.V.Babintsev et al.: IHEP M-25 (1976);
100.0 GeV/c, J.Erwin et al.: Phys. Rev. Lett. 32 (1974) 254;
100.0 GeV/c, W.M.Morse et al.: Phys. Rev. D15 (1977) 66;
100.0 GeV/c, A.E.Brenner et al.: Phys. Rev. D26 (1982) 1497;
102.0 GeV/c, C.Bromberg et al.: Phys. Rev. Lett. 31 (1973) 1563;
175.0 GeV/c, A.E.Brenner et al.: Phys. Rev. D26 (1982) 1497;
205.0 GeV/c, S.Barish et al.: Phys. Rev. D9 (1974) 2689;
250.0 GeV/c, M.Adamus et al.: Z. Phys. C32 (1986) 475;
303.0 GeV/c, A.Firestone et al.: Phys. Rev. D10 (1974) 2080;
303.0 GeV/c, F.T.Dao et al.: Phys. Rev. Lett. 29 (1972) 1627;
360.0 GeV/c, J.L.Bailey et al.: CERN/EP83-192;
400.0 GeV/c, R.D.Kaas et al.: Phys. Rev. D20 (1979) 6050;
405.0 GeV/c, W.S.Toothacker et al.: UMBC77-77;
405.0 GeV/c, C.Bromberg et al.: Phys. Rev. Lett. 31 (1973) 1563;
493.0 GeV/c, A.Breakstone et al.: Phys. Rev. D30 (1984) 528;
800.0 GeV/c, R.Ammar et al.: Phys. Lett. B178 (1986) 124;
1032.0 GeV/c, A.Breakstone et al.: Phys. Rev. D30 (1984) 528;

1471.1 GeV/c, A.Breakstone et al.: Phys. Rev. D30 (1984) 528;
 2062.0 GeV/c, A.Breakstone et al.: Phys. Rev. D30 (1984) 528;
 540 GeV, G.J.Ainer et al., UA5 collaboration: Phys.Rep. 154 (1987) 247.

- [11] G.Wrochna: "Multiparticle Production as a Bivariate Branching Process", Warsaw University Preprint IPD/5/1990, to be published in the Proceedings of the XIII Warsaw Symposium on Elementary Particle Physics, Kazimierz, Poland, May 1990.
 [12] N.Arley and K.R.Buch: Introduction to the Theory of Probability and Statistics, New York 1950, Chapter 10, (John Wiley and Sons).
 [13] R.Szwed, G.Wrochna and A.K.Wróblewski: "New AMY and DELPHI Multiplicity Data and the Lognormal Distribution", Warsaw University Preprint IPD/6/1990, to be published in Mod. Phys. Lett. A.

Figure captions

Fig. 1

Parameters of the lognormal distributions fitted to each of data sets [10]. The UA5 point (full circle) is shifted left to squeeze the scale.

Fig. 2

The probit diagram for pp multiplicity distributions ranging from $\sqrt{s} = 3$ to 62 GeV.

Fig. 3

Comparison of the shapes of the lognormal scaling functions $\psi(x)$ for pp and e^+e^- interactions.

Fig. 4

The pp multiplicity distributions measured by UA5 collaboration at $\sqrt{s} = 540$ GeV. The continuous line represent the lognormal distribution fitted to these data, the dotted line — the distribution fitted to lower energy data.

Fig. 5

The dispersions D_2 , D_3 and D_4 plotted as a function of the average multiplicity for the pp data (circles) and the UA5 pp data (square). The solid lines are calculated with the lognormal distribution globally fitted to all data excluding UA5 experiment.

Fig. 6

Dependence of the average continuous multiplicity (\bar{n}) in e^+e^- and pp interactions on the available energy.

Table 1

Results of fits of the lognormal distribution to the multiplicity distributions in pp inelastic collisions.

Parameters obtained for each experimental data set are indicated in the left part of the table. At the bottom the parameters obtained for the whole collection of data (global fit) are given. In the right part of the table the goodness of the description of the individual data by the globally fitted lognormal distribution is presented.

The errors correspond to the change of χ^2 of 1.

| PLAB | \sqrt{s} | fit to the specified data set | | | | "global fit" | | | | |
|--------|------------|-------------------------------|---------------|-----|--------------|--------------|----------|-----------|-----------------|------|
| | | c | D | NDF | χ^2/NDF | NDF | χ^2 | \bar{X} | \bar{X}^2/NDF | |
| 4.0 | 3.1 | 97.37 ± 99.00 | 0.635 ± 0.030 | 1 | 0.0 | 0.00 | 3 | 5.01 | 1.67 | |
| 5.5 | 3.5 | 6.78 ± 4.05 | 0.628 ± 0.032 | 1 | 0.0 | 0.00 | 3 | 8.23 | 2.74 | |
| 6.5 | 3.8 | 3.09 ± 2.49 | 0.583 ± 0.006 | 3 | 4.3 | 1.44 | 5 | 7.07 | 1.41 | |
| 12.0 | 4.9 | 4.74 ± 0.92 | 0.531 ± 0.011 | 3 | 14.0 | 4.66 | 5 | 16.66 | 3.33 | |
| 19.0 | 6.1 | 2.33 ± 0.58 | 0.584 ± 0.011 | 5 | 6.3 | 1.26 | 7 | 29.52 | 4.22 | |
| 24.0 | 6.8 | 3.37 ± 0.52 | 0.624 ± 0.009 | 6 | 28.1 | 4.68 | 8 | 35.45 | 4.43 | |
| 35.7 | 8.3 | 3.30 ± 1.16 | 0.624 ± 0.020 | 5 | 8.2 | 1.65 | 7 | 9.59 | 1.37 | |
| 50.0 | 9.8 | 7.32 ± 7.00 | 0.654 ± 0.030 | 6 | 3.9 | 0.66 | 8 | 4.60 | 0.58 | |
| 60.0 | 10.7 | 3.77 ± 3.15 | 0.585 ± 0.035 | 6 | 2.2 | 0.36 | 8 | 7.01 | 0.88 | |
| 69.0 | 11.5 | 5.22 ± 2.16 | 0.651 ± 0.025 | 8 | 14.8 | 1.85 | 10 | 17.32 | 1.73 | |
| 100.0 | 13.8 | 3.67 ± 2.22 | 0.654 ± 0.032 | 8 | 7.0 | 0.88 | 10 | 11.80 | 1.18 | |
| 100.0 | 13.8 | 2.24 ± 2.24 | 0.637 ± 0.028 | 7 | 9.5 | 1.35 | 9 | 12.16 | 1.35 | |
| 102.0 | 13.9 | 4.35 ± 2.22 | 0.645 ± 0.026 | 8 | 7.6 | 0.95 | 10 | 9.58 | 0.96 | |
| 175.0 | 16.2 | 8.31 ± 8.81 | 0.651 ± 0.083 | 8 | 1.8 | 0.22 | 10 | 2.09 | 0.21 | |
| 205.0 | 19.7 | 3.25 ± 1.20 | 0.609 ± 0.020 | 11 | 14.9 | 1.36 | 13 | 16.74 | 1.29 | |
| 250.0 | 21.7 | 4.33 ± 1.91 | 0.665 ± 0.025 | 12 | 21.7 | 1.81 | 14 | 33.15 | 2.37 | |
| 303.0 | 23.9 | 4.01 ± 1.73 | 0.614 ± 0.021 | 12 | 15.7 | 1.31 | 14 | 17.39 | 1.24 | |
| 303.0 | 23.9 | 2.02 ± 1.13 | 0.596 ± 0.025 | 11 | 18.7 | 1.70 | 13 | 21.60 | 1.66 | |
| 360.0 | 26.0 | 2.91 ± 0.89 | 0.596 ± 0.015 | 11 | 12.5 | 1.14 | 13 | 20.32 | 1.56 | |
| 400.0 | 27.4 | 6.12 ± 2.95 | 0.648 ± 0.017 | 13 | 18.2 | 1.40 | 15 | 21.41 | 1.43 | |
| 400.0 | 27.4 | 6.00 ± 3.31 | 0.650 ± 0.029 | 12 | 23.3 | 1.94 | 14 | 24.56 | 1.75 | |
| 405.0 | 27.6 | 2.90 ± 1.01 | 0.628 ± 0.014 | 14 | 19.1 | 1.36 | 16 | 21.19 | 1.32 | |
| 493.0 | 30.4 | 6.23 ± 4.57 | 0.667 ± 0.047 | 15 | 8.8 | 0.59 | 17 | 10.77 | 0.63 | |
| 800.0 | 38.8 | 3.64 ± 1.11 | 0.614 ± 0.015 | 14 | 22.5 | 1.61 | 16 | 25.07 | 1.57 | |
| 1032.0 | 44.0 | 2.59 ± 1.15 | 0.620 ± 0.024 | 17 | 6.5 | 0.38 | 19 | 8.87 | 0.47 | |
| 1471.1 | 52.6 | 3.61 ± 1.65 | 0.597 ± 0.025 | 19 | 11.3 | 0.60 | 21 | 12.44 | 0.59 | |
| 2062.0 | 62.2 | 16.83 ± 16.83 | 0.682 ± 0.044 | 18 | 13.6 | 0.75 | 20 | 20.29 | 1.01 | |
| all | | 4.25 ± 0.20 | 0.629 ± 0.003 | — | — | — | — | 316 | 458.49 | 1.45 |
| | 540.0 | 1.12 ± 0.22 | 0.642 ± 0.011 | 38 | 29.1 | 0.77 | — | — | — | — |

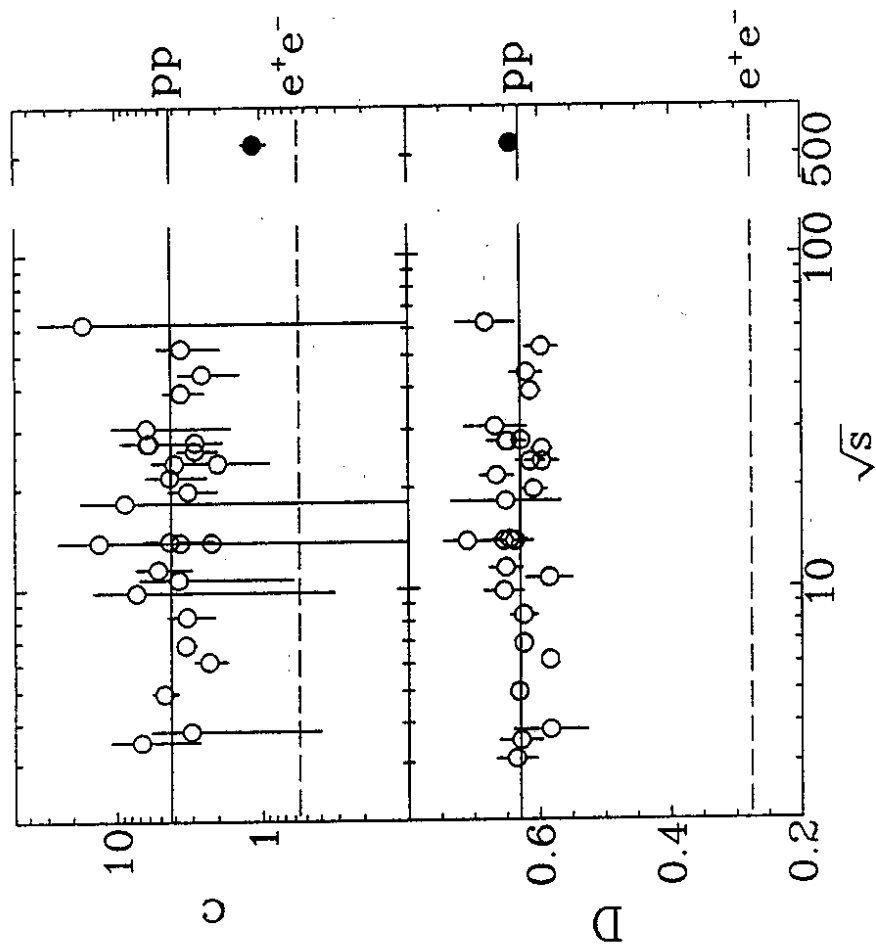


Fig.1

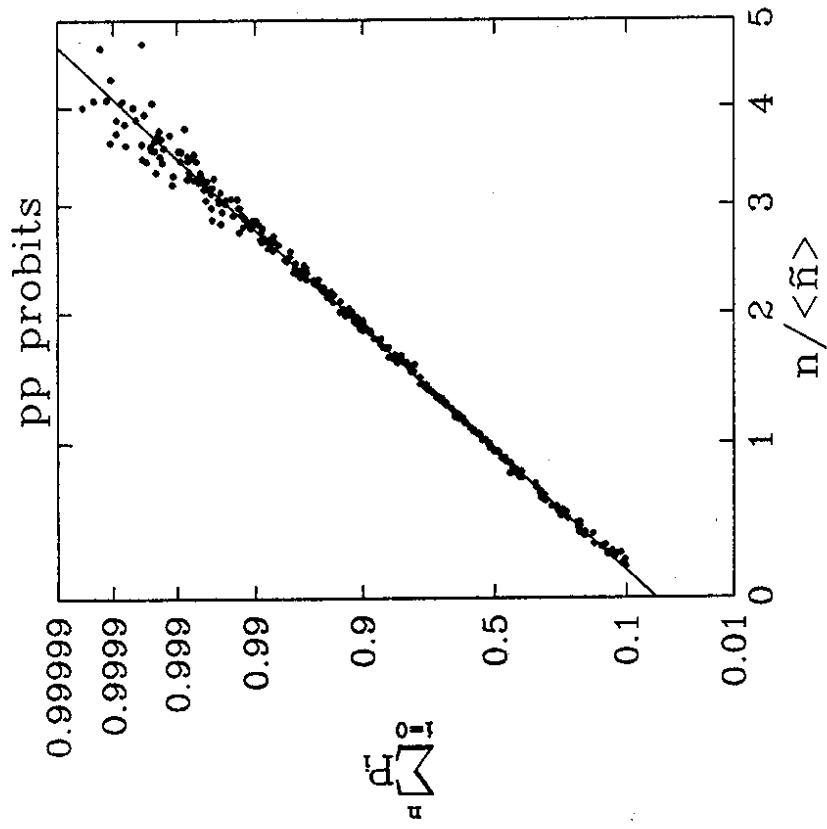


Fig.2

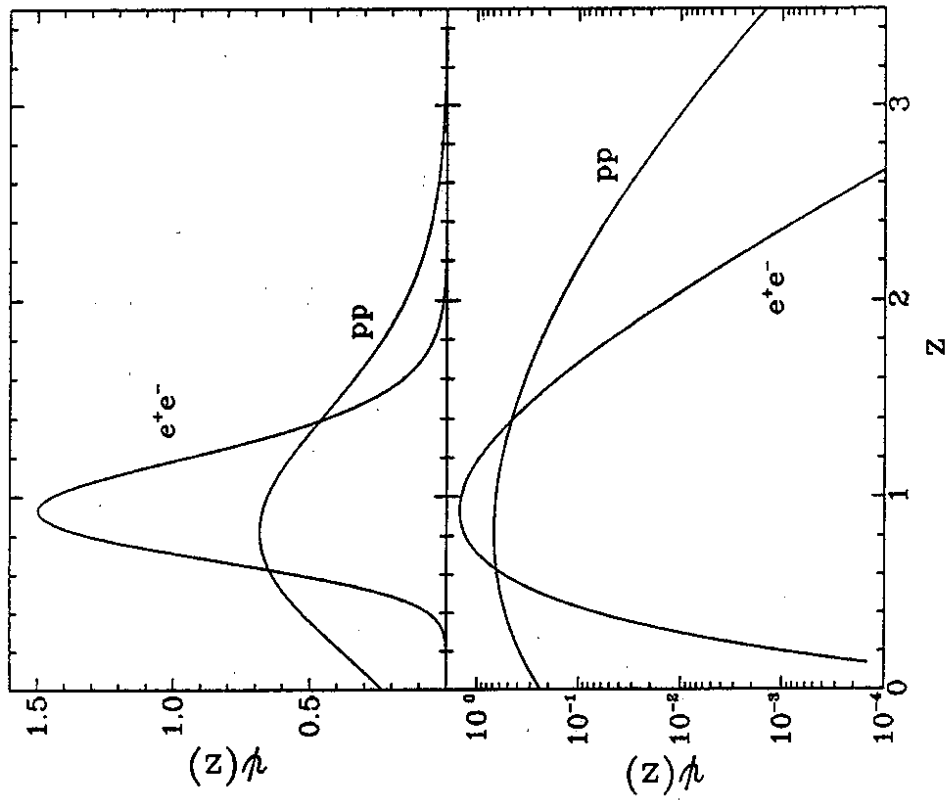


Fig.3

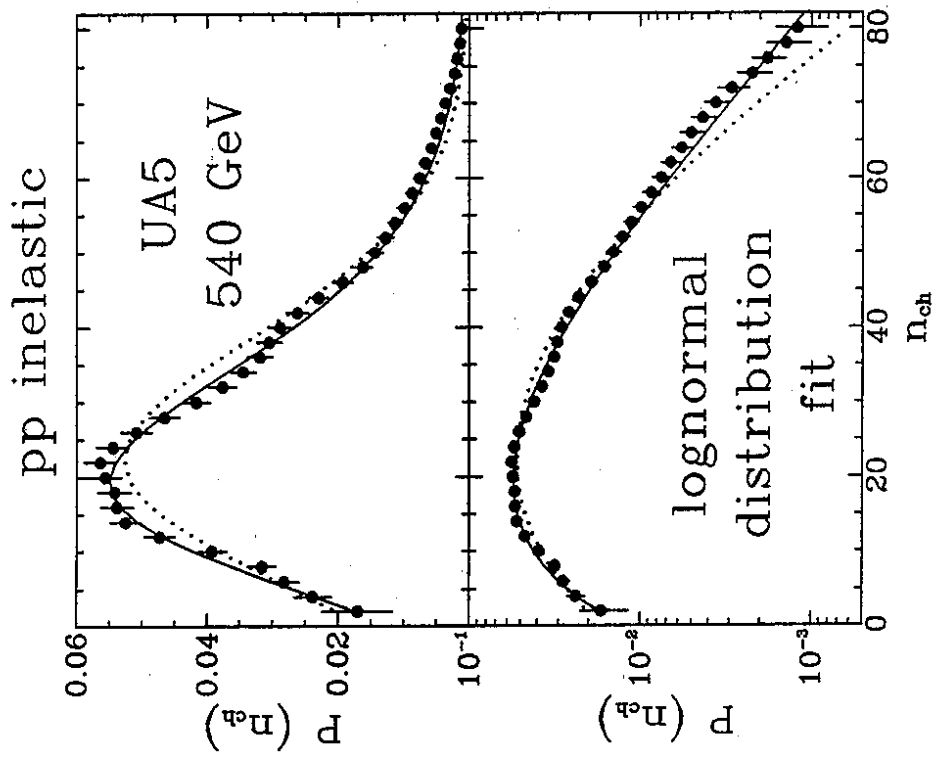


Fig.4

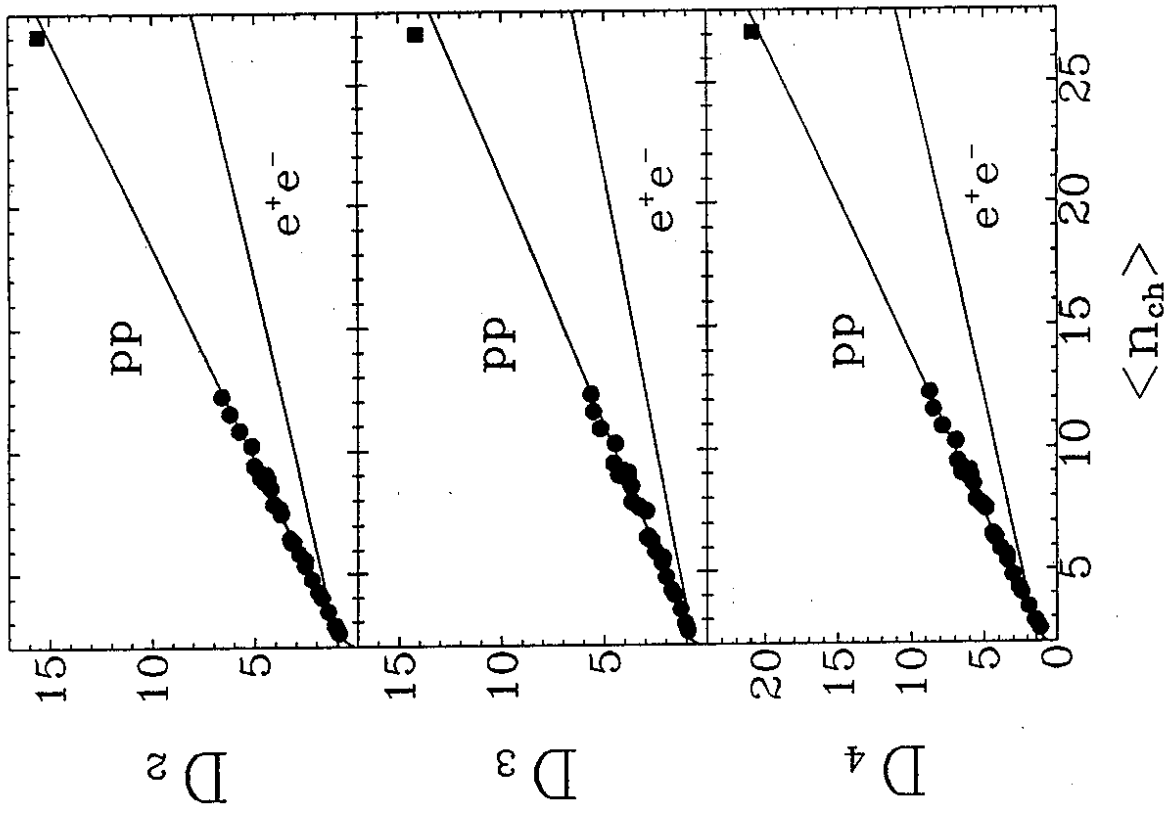


Fig.5

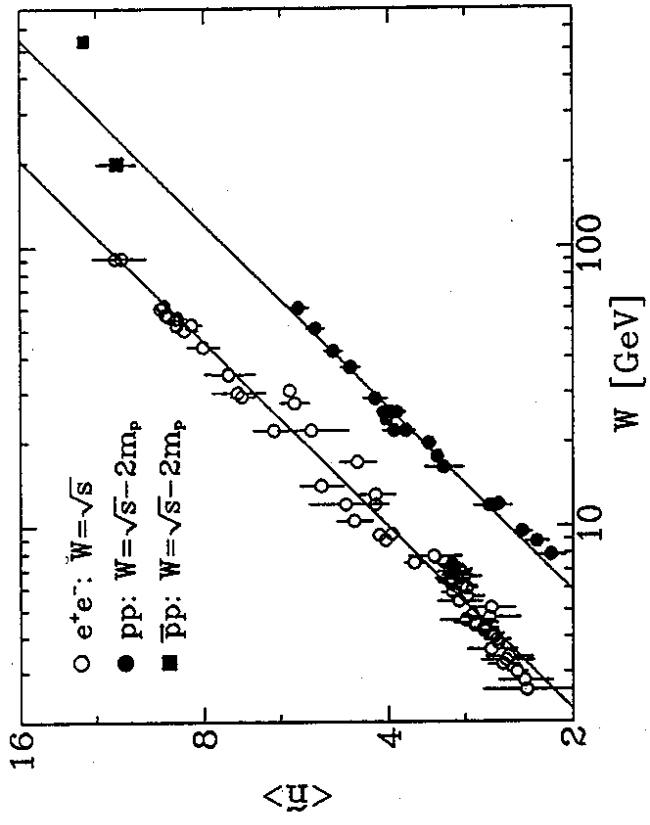


Fig.6